Article Identifier
DOI: 10.22032/dbt.58726
URN: urn:nbn:de:gbv:ilm1-2023isc-015:3

60th ILMENAU SCIENTIFIC COLLOQUIUM
Technische Universität Ilmenau, 4 – 8 September 2023
URN: urn:nbn:de:gbv:ilm1-2023isc:1

USING PHOTO-ACTIVATED LOCALIZATION MICROSCOPY (PALM) FOR IMAGING FLUOROPHORE-DOPED PHOTORESISTS

Madeline Rodenberg[1]
Lukas Jonathan Münker[2]
Rainer Tutsch[1]
Peter Jomo Walla[2]
Thomas Weimann[3]

[1]Institute of Production Metrology, TU Braunschweig
[2]Institute of Physical and Theoretical Chemistry, TU Braunschweig
[3]Department Quantum Electronics, PTB Braunschweig

ABSTRACT

Photoresists play a key role in the photolithographic process being necessary to print the structure layout of dies of microchips. Following Moore's law leads to ever smaller assemblies reaching the single-digit nanometer range. Typical methods for quality assurance are scatterometry and atomic force microscopy facing challenges and disadvantages. Since overcoming the Abbe limit via superresolution techniques fluorescence microscopy can be another approach. This article describes the measurement analyses done with PALM/STORM on lithographical produced samples of positive resist doped with Atto 565. Lines with 200 nm thickness and equal spacing were studied. Thereby, ThunderSTORM provided better results than QuickPALM for data analysis. For the first experiment, using a permanently switched on 405 nm laser beam with low intensity shows the best resolution results. A rotating lambda half-wave plate in the second experiment leads to a slight increase of data quality. Further studies combining these two approaches will be carried out.

Index Terms - photoresist, superresolution microscopy, fluorescence imaging, photo-activated localization microscopy (PALM), stochastic optical reconstruction microscopy (STORM)

1. INTRODUCTION

For printing the layout for the electrical wires on a microchip's surface photoresists play a key role in the photolithographic process and thus in the electronic semiconductor industry [1]. Since the discovery of "Bakelite" by Leo Hendrik Baekeland at the beginning of the 20th century a lot of development has taken place [1]. From the early days of combining novolak as the resin and diazonaphthoquinone (DNQ) as the light-active component, various resist compositions have since emerged to meet different process requirements [1]. In addition, following Moore's law, the size of printed structures has been continually reduced whereas in contrast the density of components on a circuit board has increased, leading to structures designs in the single-digit nanometer range printed today via deep ultraviolet light lithography [1].
Checking these structures for quality assurance can consequently become a challenge. Typical methods are scatterometry or a photo mask inspection done with atomic force microscopy (AFM) [2]. Both measurement methods have advantages and disadvantages such as high costs

[3]. Furthermore, an analysis done with an AFM takes a lot of time resulting in long intervals between each mask scan. Also, this technique can cause a destruction of the sample [3]. Another approach is therefore the use of optical microscopy to analyze the printed structures as inline measurement system during the lithographic process.
For a long time, optical microscopy could not be used for investigating nanostructures due to Abbe's limit. Since the development of superresolution techniques like stimulated emission depletion (STED), photo-activated localization microscopy (PALM) and stochastic optical reconstruction microscopy (STORM) this limit has been overcome [4]. While STED is based on a confocal fluorescence microscope which scans the sample, PALM/STORM uses a wide-field microscope. Thereby, both methods rely on the principle of stochastic blinking of the fluorescence molecules. PALM uses photoconvertible or photoactivatable fluorescent protein molecules, whereas the synthetic photoswitchable fluorophores are used as probes in a STORM experiment [5]. Today, superresolution imaging approaches based on illumination by STED as well as the probe-based methods of PALM and STORM allow biochemists to visualize biological structures on a sub-diffraction limited level and thus gaining knowledge on questions relating to molecular processes in cells and organisms [5].
This leads to the idea to dope the photoresists with fluorescent dyes and analyze structures and surfaces with the help of superresolution microscopy, in our case PALM/STORM. This article describes the preliminary results on experiments carried out with Atto 565 doped positive resist (AR-P 6200.04). Layers of this solution were spun onto a microscopy glass and structures were lithographically imprinted. Subsequently, the recorded image stacks are analyzed with two algorithm variants of Henriques et al. (QuickPALM) [6] and Ovesný et al. (ThunderSTORM) [7] and their reconstructed images are compared. The blinking activity of the fluorescence molecules as a result of different pulses is investigated using a 405 nm laser beam. Furthermore, it will be followed whether the approach of incorporating a rotating lambda half-wave plate has an impact on the resolution of the data [8].

2. METHODOLOGY

2.1 Sample preparation

10 µL of a solution of Atto 565 (Atto Tec, 10^{-4} mol/L) in ethanol (denatured, > 99.8 %, with about 1 % MEK, Carl Roth) were diluted in 990 µL of AR-P 6200.04 (Allresist). Around 500 µL of this solution were dripped on a microscopy cover slip (borosilicate glass, 0.13 - 0.16 mm thickness, 22 x 22 mm, Carl Roth) in PTB's clean room centre. Then, the typical lithographic process takes place: spin coating the resist dye mixture on the cover slip at 4000 rpm for 45 s, placing the glass slip onto a hot plate (150 °C) for 1 min until all the solvent had evaporated and a thin solid resist dye layer was left. For electrical conductivity, a thin coating layer of AR-PC 5090.02 ("Electra", Allresist) was also spun onto the slip for 90 s with 2000 rpm. Again, the cover slip was placed onto the hot plate for 3 min at 90 °C to evaporate the solvent. Structures were printed into the coatings by electronic beam lithography (EBPG 5200). Afterwards, the Electra coating was removed by flushing the microscopy cover slip for 1 min under water and blowed dry. The development was done by bathing the glass slip in AR 600-546 for 1 min, and the reaction was stopped by placing it in a bath with AR 600-60 for 30 s, rinse again under water for 30 s and finally drying the sample by blowing.

As oxygen scavenging system, a stock solution of 20 mL Glox buffer was produced. It contained the components listed in Table 1:

Table 1: Substances and their concentrations of the produced Glox buffer

TN buffer	50 mM Tris pH 8.0
	10 mM NaCl
Oxygen scavenger system	0.5 mg / ml Glucose oxidase
	40 µg / ml Catalase
	10 % (weight / volume) Glucose

2.2 Designing the structures of the samples

20 rows of structures were printed on the microscopy cover slip. Each row contains fields of different sizes defined by the scale bar displayed in each section at the bottom right. Scale bars vary from 500 µm to 200 µm, 100 µm, 50 nm to 20 nm. This determines the periodicity as well as thickness of and spacing between the lines in the respective fields. Figure 1 shows a 200 µm scale bar field. On the left, are a square and a triangle. Above the triangle are two stars filled with very small and connected snowflakes, one is the positive image and the other the negative image. In the middle of each field are a circle and three scales with different pitch. The right contains the scale bar, a siemens star and three sections of lines where the line thickness equals the space between these lines (Figure 1 zoomed in sections).

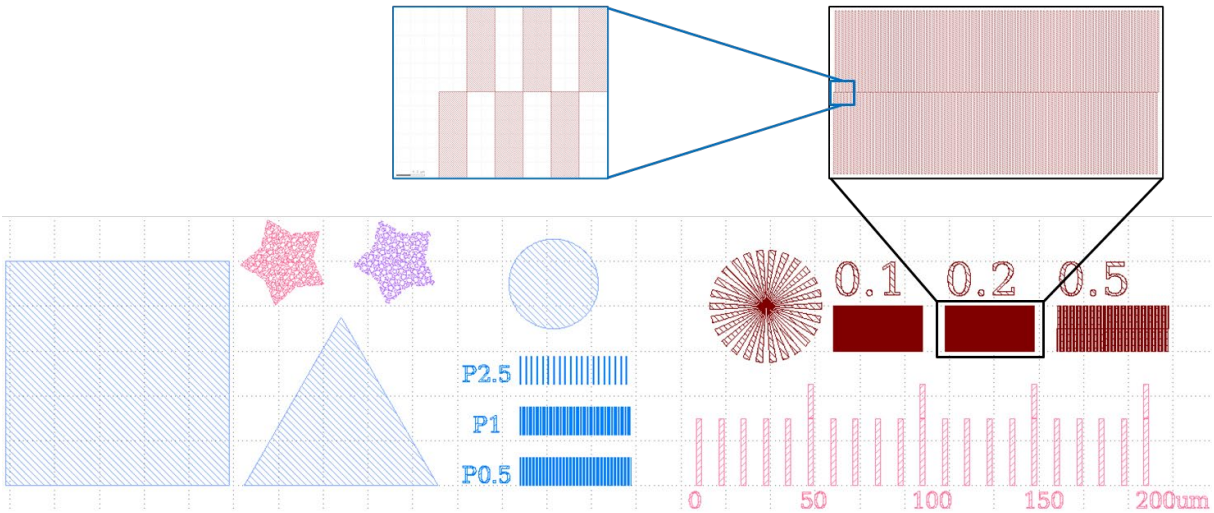

Figure 1: Printed structure design. The 200 µm scale bar field is shown. Simple structures like square, triangle and circle allow the analysis of etch effects, siemens star and lines enable resolution measurements. Note, that the lines left of the scale bar have defined periodicities, whereas the lines above the scale bar equal in line thickness and spacing between the lines. In this article, lines of 200 nm thickness and 200 nm space between the lines are under investigation and therefore shown in more detail. Freeform structures of stars filled with very tiny and connected snowflakes are also included in each field.

With this variety of forms different measurement goals can be achieved. For example, the edges of the large square, triangle and circle are used to analyze etch effects. On the other hand, resolution determinations were carried out with the help of siemens stars and the lines with defined thickness and periodicity.
For this article, we investigated lines with 200 nm thickness and spacing to compare the performances of the two used algorithms QuickPALM and ThunderSTORM as well as the impact of a rotating lambda half-wave plate on the resolution. Furthermore, it is shown that the Abbe limit has been overcome.

2.3 Measurement setup and principle

The used setup was a self-built wide-field epifluorescence microscope. A simple schematic drawing is shown in Figure 2. For exciting the fluorophore molecules, a 568 nm continuous

wave laser beam (Sapphire 568-100, Coherent) was used and for their activation, a 405 nm continuous wave laser beam (LBX-405-50, Oxxius, Laser 2000). The 405 nm laser beam is thereby coupled into the 568 nm laser beam by a dichroic mirror (long pass filter 568, AHF). Both beams were widened by a telescope system (achromatic doublets, f = 40 mm and f = 400 mm, Thorlabs) and the peripheral part was blocked by an iris diaphragm. Thus, only the central part (diameter of about 1 cm) is allowed to pass through. Afterwards, the beam was reflected by four silver mirrors, then passed a lambda quarter-wave plate (Achromatic λ/4 plate, 400–700 nm, Newport) generating circularly polarized light and a lens (achromatic doublet, f = 400 mm, Thorlabs) to focus the light onto the back focal plane of the objective. A dichroic mirror (long pass filter 568, AHF) reflected the beam towards the objective (NA = 1.40 oil immersion objective, UPlanSApo, 100x, Olympus) with both mounted into an inverted microscope body (IX50, Olympus). The fluorescence of the sample is collected by the same objective and transmitted by the aforementioned dichroic mirror. Another mirror reflected the light through two filters (568 LP edge basic long pass filter, AHF and band pass filters, 590/20, AHF) and a lens (LC 1120-A-ML, f = 100 mm, Thorlabs) towards the electron-multiplying charge coupled device camera (EMCCD, IXON-L-897 back-illuminated, Andor Technology) which recorded the signal with a frame rate of 50 fps.
The rotating lambda half-wave plate (achromatic λ/2 plate, 400–800 nm, Thorlabs) is optimally coupled into the light path between the fourth silver mirror and the achromatic doublet lens before the objective.

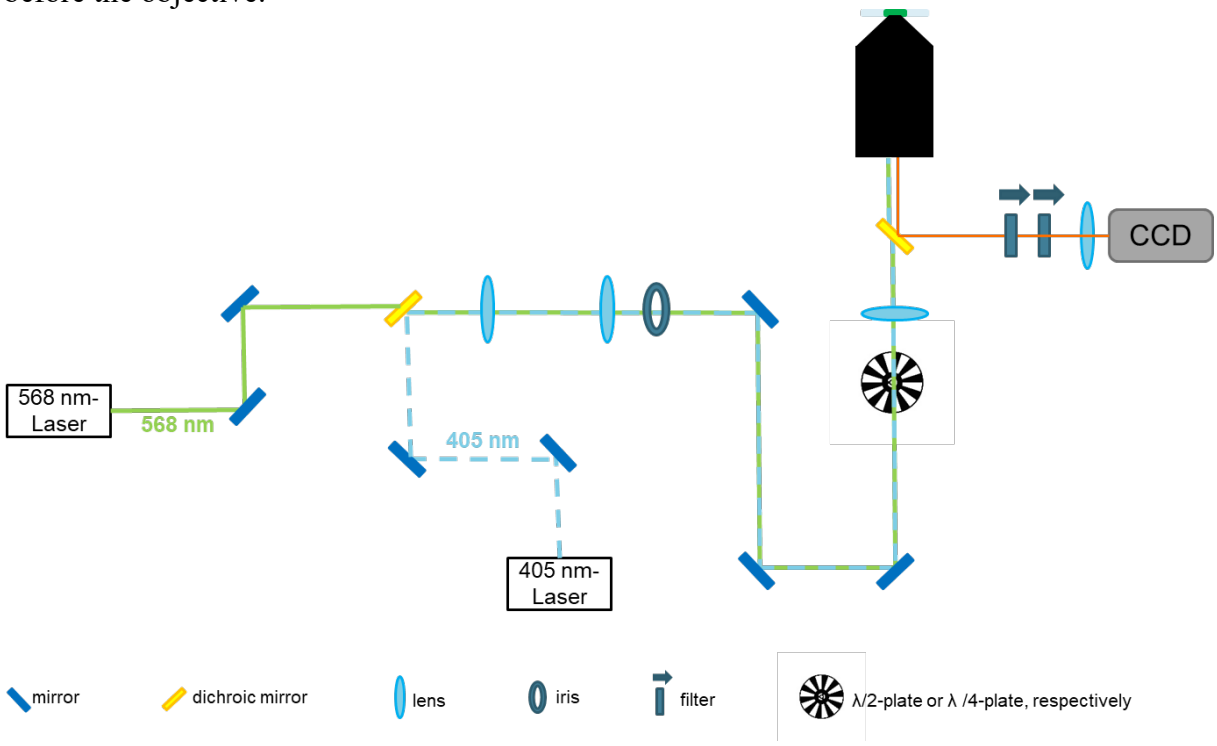

Figure 2: A schematic drawing of the PALM/STORM setup. Note, that for simplicity not all optical components are displayed here.

2.4 Measurement procedure

The first experiment investigated the impact of the 405 nm laser beam pulse on the blinking activity of the fluorescent dye molecules. Therefore, three measurement settings were performed: at the first recording, only the excitation laser beam was used and no 405 nm laser beam pulse was done. For the second video, the 405 nm laser beam was permanently switched on with a set power of 0.4 mW. In the third measurement, the activation laser was switched on after every 1000 frames for a duration of 100 frames, and a power at the laser of 6.3 mW was set.

Another experiment was done to discover any impact of the rotating lambda half-wave plate on the resolution of the imaging technique. Therefore, a reference recording without rotating wave plate was performed and compared to a measurement using the rotation wave plate. The synchronization of a chopper wheel (Optical Chopper System, Thorlabs) to the electron-multiplying charge-coupled device (EMCCD) camera achieves the rotation of the wave plate. Note, that in this case no 405 nm laser beam pulse was activated.
The 568 nm excitation laser beam was set to 100 mW in every recording run. For each measurement, an image stack of 10000 frames was captured, each frame was exposed for 20 ms. 400 µL Glox buffer was pipetted onto the glass cover slip before the experiments started.

2.5 Roadmap for data analysis

Data analysis was done in FIJI, also known as ImageJ2. Both algorithms used for this article, QuickPALM and ThunderSTORM, are plugins for the Java based image processing software.
At first, the image stacks were gaussian filtered (σ = 8) to delete global modulation and afterwards averaged images were generated.
For data analyses with QuickPALM, the filtered image stacks were used. Reconstructed high resolution images were generated via the formulas described [6] and the parameter settings shown in Table 2:

Table 2: Parameter settings implemented in the QuickPALM parameter settings menu for the image analysis

Parameter	Entered value
Minimum SNR (signal to noise ratio)	3.00
Maximum FWHM (full width half maximum) (in px)	8
Image plane pixel size (nm)	67.00
Local threshold (% maximum intensity)	45
Maximum iterations per frame	200
Threads (each takes ~3*[frame size] in memory)	16

The image reconstruction by ThunderSTORM was carried out with raw data sets. The respective formulas on coordinate calculations and so forth are described in [7] in detail. Table 3 shows input data of the used camera settings.

Table 3: Specifications of the camera setup implemented in the ThunderSTORM menu for the image analysis

Parameter	Entered value
Pixel size (nm)	67.0
Photoelectrons per A/D count	4.61
Base level (A/D counts)	100.0
EM gain	600.0

3. MEASUREMENT RESULTS

3.1 Comparing two algorithms for data analysis: QuickPALM vs. ThunderSTORM

A comparison of the both reconstructed images gained by QuickPALM and ThunderSTORM to the mere averaged picture demonstrates a large resolution increase of the recorded structures. Figure 3 shows the resulting images of the three analysis methods. The image frame contains a block of lines, 200 nm thick and 200 nm wide interstices. On the left, the individual lines are indistinguishable in the averaged image of the image stack. The reconstructed images by QuickPALM and ThunderSTORM, on the other hand, allow the individual lines to be distinguished already with the naked eye (Figure 3, (c) and (e)). Thus, demonstrating that the

Abbe limit has been overcome. This is also illustrated by the profile plots: The diagram in (b) shows a very broad curve in which several lines appear to be combined into larger amplitudes. In contrast, the individual 200 nm lines in (d) and (f) are visible as fine curves with increased frequency. It should be noticed, that the curve etches in (f) seem to be less noisy than in (d) leading to the conclusion that the ThunderSTORM algorithm achieves the better results. This is in good agreement to Ovesný et al. [7].

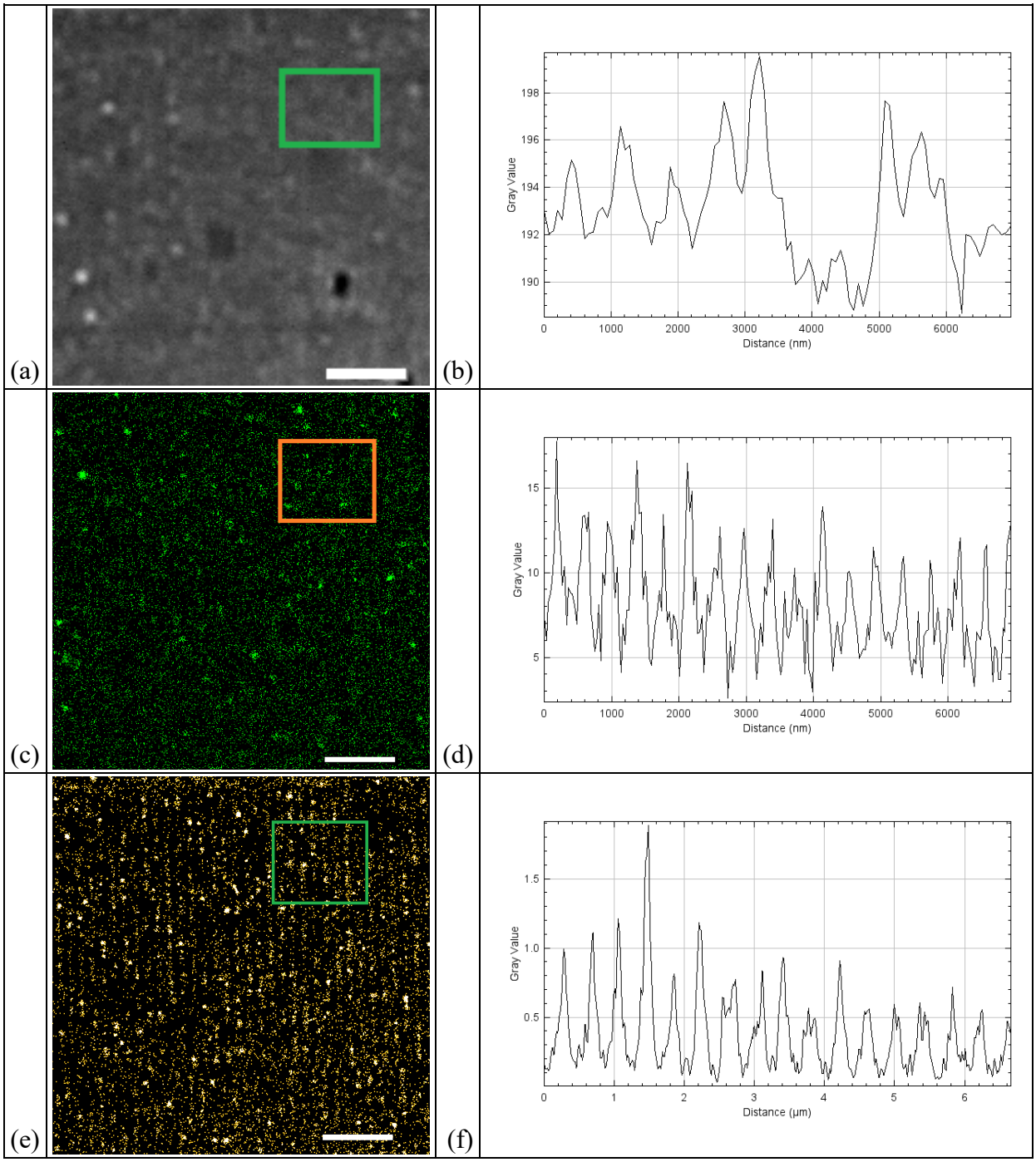

Figure 3: Lines with 200 nm thickness and distance become visible with the help of PALM/STORM. (a) shows the averaged picture of a 10000 frames image stack. The stack was then analyzed with the two ImageJ plugins QuickPALM and ThunderSTORM whose reconstructed images are demonstrated in (c) and (e), respectively. The green and orange rectangles in (a), (c) and (e) mark the fields of the profile plots which are displayed in (b), (d) and (f). To counteract possible outliers, the data in the highlighted rectangles was averaged in vertical direction. Scale bars, 2.5 µm.

Possible reasons for this effect may be an erroneous determination of the FWHM or the inaccurate specification of the signal to noise ratio. Further investigations are therefore still pending.

3.2 The impact of the 405 nm laser beam pulse

Another series of measurements compared different pulse approaches of the 405 nm laser beam with the blinking activity of the Atto 565 molecules. After some time, fluorescent molecules can bleach, especially since the sample is illuminated with relatively high laser power. To reactivate these molecules from the dark state, the 405 nm laser pulse is used.

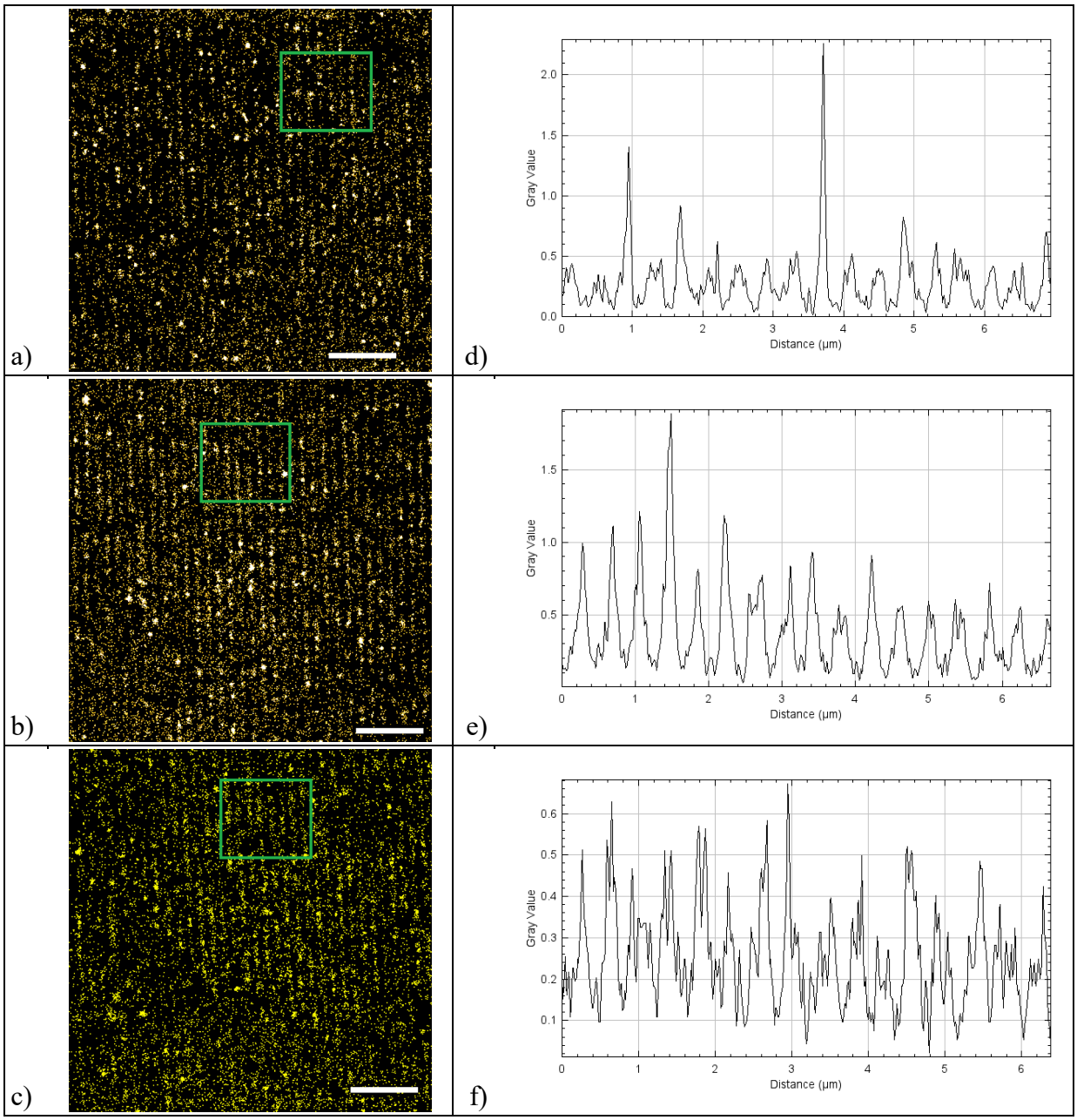

Figure 4: Via ThunderSTORM reconstructed images of lines of 200 nm thickness and 200 nm wide interstices (a - c) as well as the respective profile plots (d – f). (a) is the reference image where the recording was performed without 405 nm laser beam pulse. (b) 405 nm laser beam was permanently switched on with a set laser power of 0.4 mW (7 % of the current). (c) is done with a 405 nm laser beam pulse every 1000 frames for a duration of 100 frames with a set power of 6.3 mW (25 % of the current). Again, the green rectangles in (a - c) mark the fields of the profile plots displayed in (d - f) whose data was averaged in vertical diraction. Scale bars, 2.5 µm.

Figure 4 shows the reconstructed images analyzed by ThunderSTORM as well as the respective profile plots of the aforementioned 200 nm lines recorded without any 405 nm laser beam usage (a), a permanently added 405 nm laser beam with 0.4 mW (b) and recurring switch on after 1000 frames for a duration of 100 frames with power set at 6.3 mW (c). Again, separated lines can be determined with naked eyes. A closer look at the profile plots indicates that the use of the activation laser definitely increases the resolution, since the amplitudes have increased as a result of its use compared to reference measurement without 405 nm laser beam. The signal intensity is in (d) about 0.5, in (e) around 0.8 and in (f) 0.6. Furthermore, the plots indicate an improvement of the signal to noise ratio when the activation beam is continuously switched on at low power settings.

3.3 The impact of the rotating lambda half-wave plate

The last experiment in this article investigates the impact of a rotating lambda half-wave plate on the resolution of the image data. Comparing the reconstructed images by QuickPALM and ThunderSTORM in Figure 5 indicates an increase of detected molecules when using the rotating lambda half-wave plate. This is due to the fact that a fluorophore is converted to the excited state when its dipole moment is parallel to the polarization vector. By rotating the polarization vector more molecules likely absorb the exciting light and thus, more blinking events occur and can be detected [8]. This also leads to a slide increase of the signal to noise ratio when comparing the respective profile plots. But to make a reliable statement further research has to be done.

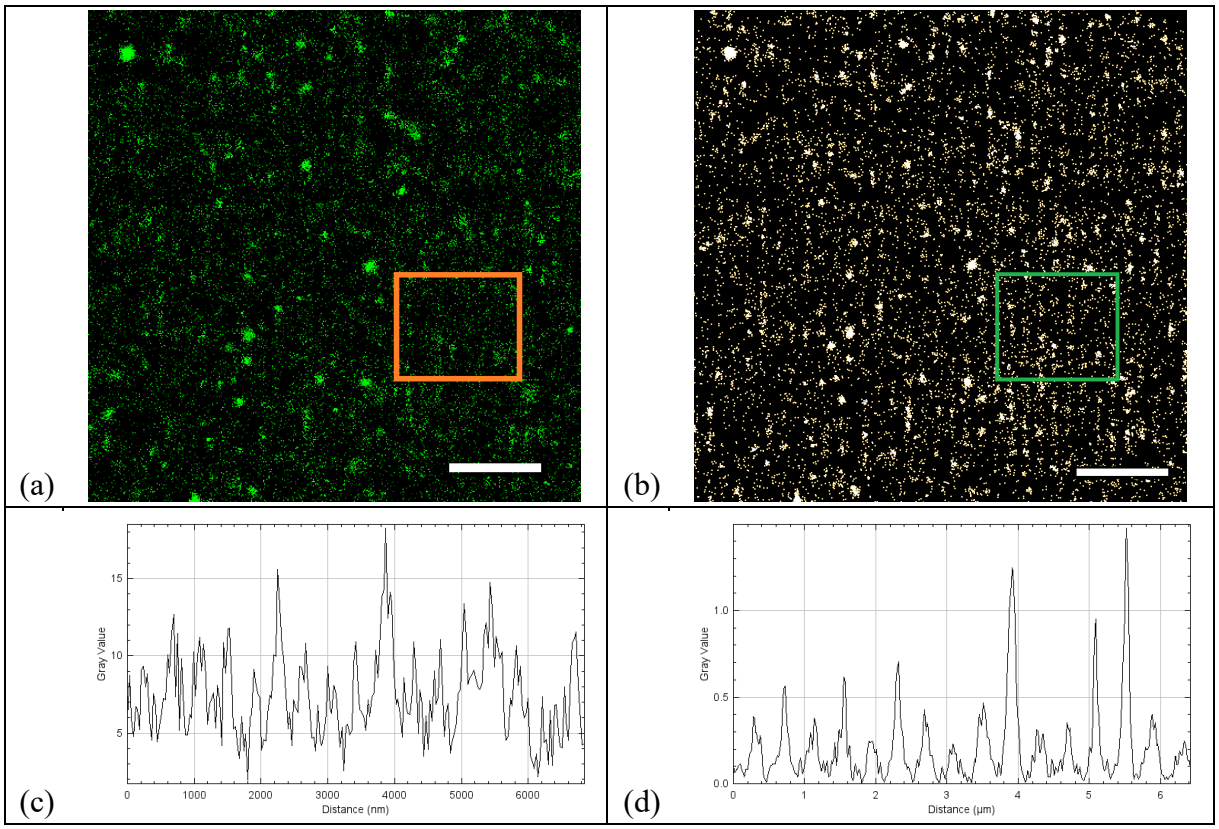

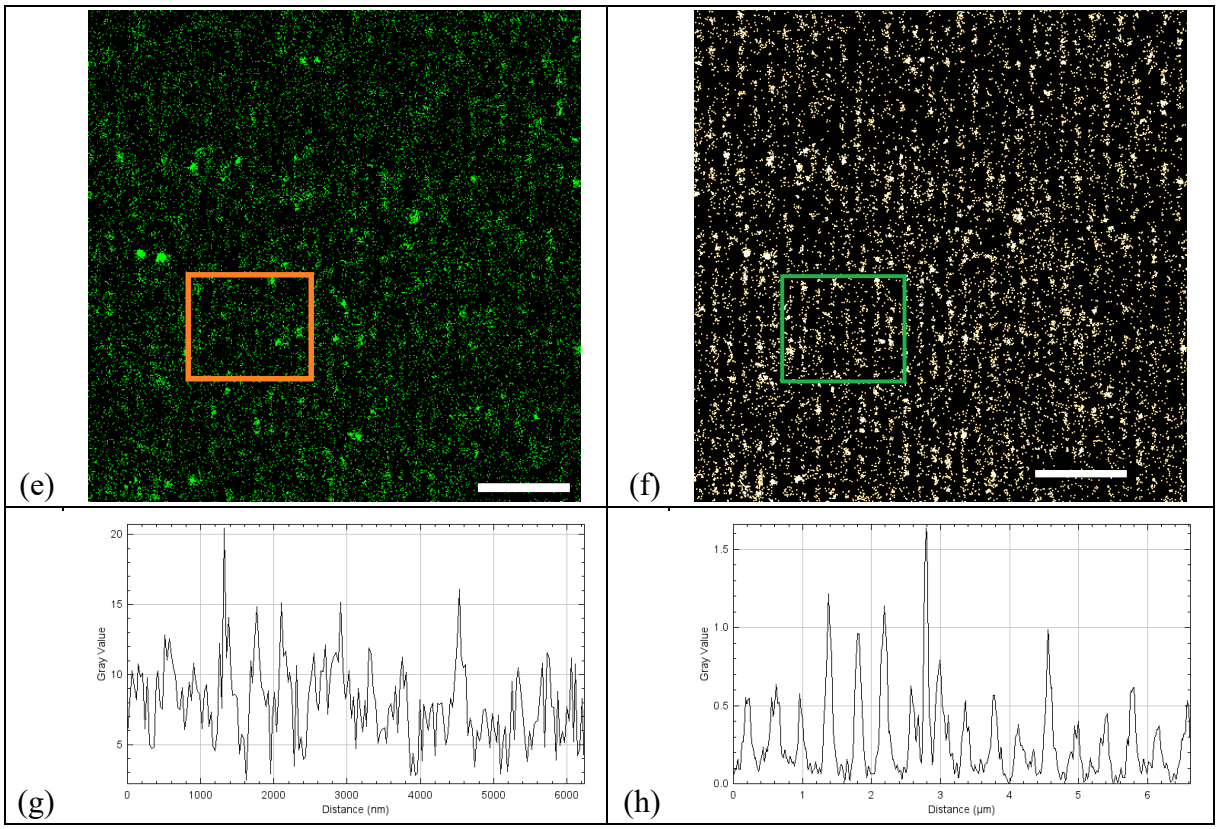

Figure 5: Again, lines with 200 nm thickness and distance, reconstructed pictures of a 10000 frames stack recorded without using the rotating lambda half-wave plate by QuickPALM (a) and ThunderSTORM (b) and the respective profile plots of the orange and green marked square field (c - d) and the corresponding reconstructed pictures (e – f) as well as the profile plots (g – h) of recordings with the use of the rotating lambda half-wave plate. Note, that no 405 nm laser pulse was used here. Scale bars, 2.5 µm.

4. CONCLUSION

In this article, we studied technical produced samples using biochemical analyzing approaches. The chosen measurement method in this case is the superresolution fluorescence microscopy PALM/STORM. Therefore, a positive photoresist (AR-P 6200.04) was doped with the fluorophore Atto 565. Following the lithographic process, the solution was spun onto a microscopy cover slip. Afterwards, structures were printed into the coating and developed. To prove that structures below the resolution limit can be investigated, image stacks (10000 frames) of lines 200 nm thickness 200 nm wide interstices were acquired. Data analysis was performed using two algorithms: QuickPALM and ThunderSTORM, with the latter leading to better results. Two series of experiments were performed. The first analyzed the impact of a 405 nm laser beam pulse on the blinking activity of the fluorescent dyes. This is possible due to the fact that the bleached molecules can be reactivated from the dark state by this pulse. It was found that the best results were obtained when the laser beam was switched on permanently at low power (0.4 mW). In the second experiment, the effect of a rotating lambda half-wave plate on the data quality and thus the resolution of the structures was measured. The rotation of the polarization vector leads to a greater number of molecules being excited resulting in small increase in resolution. Additional studies will be carried out combining the two analyzing approaches to further increase the resolution of the reconstructed images of the structures.

5. ACKNOWLEDGEMENTS

We gratefully acknowledge the support of the Braunschweig International Graduate School of Metrology B-IGSM and the DFG Research Training Group 1952 Metrology for Complex Nanosystems.

REFERENCES

[1] S. Globisch, Lehrbuch Mikrotechnologie für Ausbildung, Studium und Weiterbildung, 1st Ed., Carl Hanser Verlag, München, 2011.
[2] H.J. Levinson, Principles of lithography, 3rd Ed., Society of Photo-optical Instrumentation Engineers, Bellingham Washington, 2010.
[3] R. Doering, Y. Nishina, Handbook of semiconductor manufacturing technology, 2nd Ed., Taylor & Francis, London, 2008.
[4] P.J. Walla, Modern Biophysical Chemistry, 2nd Ed., Wiley-VCH, Weinheim, 2014.
[5] G. Patterson, M. Davidson, S. Manley, and J. Lippincott-Schwartz, "Superresolution Imaging using Single-Molecule Localization", Annual Review of Physical Chemistry, Annual Reviews, pp. 345-367, 2010.
[6] R. Henriques, M. Lelek, E. F. Fornasiero, F. Valtorta, C. Zimmer, and M. M. Mhlanga, "QuickPALM: 3D real-time photoactivation nanoscopy image processing in ImageJ", Nature Methods, pp. 339-340, 2010.
[7] M. Ovesný, P. Křížek, J. Borkovec, Z. Švindrych, and G. M. Hagen, "ThunderSTORM: a comprehensive ImageJ plug-in for PALM and STORM data analysis and super-resolution imaging", Bioinformatics, pp. 2389-2390, 2014.
[8] N. Hafi, M. Grunwald, L.S. van den Heuvel1, T. Aspelmeier, J.-H. Chen, M. Zagrebelsky, O.M. Schütte, C. Steinem, M. Korte, A. Munk, and P.J. Walla, "Fluorescence nanoscopy by polarization modulation and polarization angle narrowing", Nature Methods, pp. 579-584, 2014.

CONTACTS

M.Sc. M. Rodenberg
email: m.rodenberg@tu-braunschweig.de
ORCID: https://orcid.org/0009-0008-8945-7328

Prof. Dr.-Ing. R. Tutsch
email: r.tutsch@tu-bs.de
ORCID: https://orcid.org/0000-0003-0940-379X